

Stack Transformer Based Spatial-Temporal Attention Model for Dynamic Sign Language and Fingerspelling Recognition*

Koki Hirooka[†] Abu Saleh Musa Miah* Tatsuya Murakami*

Md. Al Mehedi Hassan[‡] Yong Seok Hwang[§] Jungpil Shin*¶

Abstract

Hand gesture-based Sign Language Recognition (SLR) serves as a crucial communication bridge between deaf and non-deaf individuals. While Graph Convolutional Networks (GCNs) are common, they are limited by their reliance on fixed skeletal graphs. To overcome this, we propose the Sequential Spatio-Temporal Attention Network (SSTAN), a novel Transformer-based architecture. Our model employs a hierarchical, stacked design that sequentially integrates Spatial Multi-Head Attention (MHA) to capture intra-frame joint relationships and Temporal MHA to model long-range inter-frame dependencies. This approach allows the model to efficiently learn complex spatio-temporal patterns without predefined graph structures. We validated our model through extensive experiments on diverse, large-scale datasets (WLASL, JSL, and KSL). A key finding is that our model, trained entirely from scratch, achieves state-of-the-art (SOTA) performance in the challenging fingerspelling categories (JSL and KSL). Furthermore, it establishes a new SOTA for skeleton-only methods on WLASL, outperforming several approaches that rely on complex self-supervised

pre-training. These results demonstrate our model's high data efficiency and its effectiveness in capturing the intricate dynamics of sign language. The official implementation is available at our GitHub repository: <https://github.com/K-Hirooka-Aizu/skeleton-slr-transformer>.

Keywords: Hand Pose, Sign Language Recognition (SLR), Japanese Sign Language (JSL), Korean Sign Language (KSL), Large Scale Dataset, Spatial-Temporal Attention, Deep Learning Network.

1 Introduction

According to the World Health Organization (WHO) [1], over 430 million people worldwide—more than 5% of the global population—require rehabilitation to address disabling hearing loss, and this number is expected to rise to over 700 million by 2050. Automatic Sign Language Recognition (SLR) has therefore emerged as a socially impactful research field dedicated to bridging the communication gap between Deaf and hearing individuals. Sign language (SL), the primary communication medium for the Deaf community, is a visual-spatial language characterized by its own grammar and lexicon. It conveys meaning through a combination of manual components—such as hand shapes, body postures, and movements—and non-manual elements like facial expressions and head motions. Core tasks in Sign Language Understanding (SLU) include Isolated Sign Language Recognition (ISLR) for word-level recognition, Continuous Sign Language Recognition (CSLR) for recognizing continuous sign sequences, and Sign Language Translation

*This paper is currently under review for possible publication in IEEE Access.

[†]School of Computer Science and Engineering, The University of Aizu, Aizuwakamatsu 965-8580, Japan. (e-mail: {s1280138, jpshin}@u-aizu.ac.jp; m-abu@u-aizu.ac.jp; t-murakami@u-aizu.ac.jp)

[‡]Research Institute for Electronic Science (RIES), Hokkaido University, Japan.

[§]Department of Electronics Engineering, Kwangwoon University, Seoul 01897, South Korea. (e-mail: thestone@kw.ac.kr)

¶Corresponding authors: Jungpil Shin, Yong Seok Hwang

(SLT) for generating spoken-language translations.

Currently, due to the rapid advancement of deep learning, various automatic sign language recognition systems are being developed. The data modalities used in sign language research can be broadly categorized into vision-based and sensor-based modalities. Sensor-based modalities capture human motion directly using wearable devices attached to the body. This approach is generally less affected by environmental factors and often achieves higher accuracy compared to vision-based methods. However, due to the inconvenience of wearing sensors and the high cost of the equipment, sensor-based approaches are not well-suited for practical real-time applications. In contrast, vision-based modalities collect data using visual sensors such as cameras. This approach offers advantages in terms of lower cost and greater suitability for real-time applications. Furthermore, various models have been proposed within the vision-based modality, depending on the type of input data such as RGB, depth, and skeleton. Specifically, skeleton-based data is typically modeled using graph neural networks (GNNs) or graph convolutional networks (GCNs). These are well-suited for capturing the spatial and structural relationships between joints in the body, and the development of skeleton-based human action recognition and sign language recognition models, spearheaded by Spatial Temporal Graph Convolutional Networks (ST-GCN) [2], is advancing rapidly. Li et al. [3] have proposed different models for sign language recognition tasks depending on the data modality. For RGB data, they introduced approaches that combine 2D Convolutional Neural Networks (2D CNNs) with Gated Recurrent Units (GRUs) [4], as well as methods based on Inflated 3D ConvNets (I3D) [5]. For skeleton data, they also proposed models employing GRUs and pose-based temporal graph convolution networks (Pose-TGCN) to effectively capture temporal dynamics and spatial relationships among joints. Liu et al. [6] have proposed a channel-wise Graph Neural Network (GNN) that uses Channel-wise Topology Refinement Graph Convolution (CTR-GC) [7] as its core backbone. This network has multi-scale recognition capability and performs temporal reweighting for each keypoint. Furthermore, the Hu et al. [8, 9] have proposed an integrated model that employs a Graph

Convolution Network for gesture state embedding and spatial embedding, and a BERT [10] to capture temporal context.

The reason GCN continues to be adopted lies in its ability to incorporate the human body's structural prior knowledge as an "inductive bias" into the graph structure model, enabling efficient learning. However, these models inherently possess limitations stemming from their reliance on fixed structures, which form the foundation of their success. The physical skeletal graphs used in GCNs struggle to directly capture the relationships between joints that are physically distant yet semantically strongly connected, such as the hands and head during actions like "clapping" or "making a phone call." Consequently, their ability to model coordinated whole-body movements and context-dependent dynamic interactions between joints is limited, contributing to a plateau in recognition accuracy.

To overcome the limitations of fixed graph structures inherent in GCNs, this study focuses on Transformers [11], which do not require predefined graph structures. The self-attention mechanism, the core of the Transformer, dynamically computes relationships among all joints based on the task's context, effectively modeling global, coordinated movements and long-range temporal dependencies.

Therefore, we propose Sequential Spatio-Temporal Attention Network (SSTAN), a novel Transformer-based architecture for sign language and finger-spelling recognition. Our model is built upon a post-normalization framework and is specifically designed to sequentially integrate spatial (intra-frame) and temporal (inter-frame) attention, aiming to achieve high performance across diverse sign language datasets.

The primary contributions of this study are as follows:

1. We propose a novel Transformer architecture, Sequential Spatio-Temporal Attention Network (SSTAN), which employs a post-normalization framework to sequentially integrate spatial and temporal dependencies using multi-head self-attention.
2. We demonstrate that our model achieves state-of-the-art performance on the Japanese and Korean

fingerspelling datasets, and highly competitive results on the large-scale WLASL dataset, all without the need for pre-training.

These contributions establish an effective and robust method for Sign Language Recognition (SLR), advancing the state-of-the-art by efficiently capturing complex spatio-temporal dynamics.

The presented work is organized as follows: Section 2 summarizes the existing research work and problems related to the presented work, Section 3 describes the benchmark and proposed Korean sign language datasets, and Section 4 describes the architecture of the proposed system—Section 5 demonstrated the evaluation performed with state of the art comparison. In Section 7, draw the conclusion and future work.

2 Related Work

2.1 Deep Learning-based Human Action Recognition

The field of deep learning-based human action recognition has been largely shaped by two primary data modalities: RGB video and skeleton data. Early breakthroughs were predominantly achieved using RGB-based approaches, with 3D Convolutional Neural Networks (3D-CNNs) and two-stream architectures demonstrating remarkable success in capturing both spatial and temporal features from video frames. Despite their success, these methods are computationally intensive and often sensitive to nuisance variables such as background clutter, lighting variations, and viewpoint changes. Furthermore, the use of raw video footage raises significant privacy concerns. To mitigate these challenges, skeleton-based methods have emerged as a powerful and efficient alternative. By representing human motion as a series of keypoint coordinates, skeleton data offers a compact, robust, and privacy-preserving representation that is invariant to many of the issues affecting RGB data. Given these advantages, this paper will focus its review on the evolution and state-of-the-art of skeleton-based action recognition models.

2.2 Skeleton-Based Human Action Recognition

Sign Language Recognition (SLR) is widely regarded as a specialized and challenging sub-domain of Human Action Recognition (HAR). Consequently, many techniques initially developed for general HAR have been adapted for SLR. However, SLR presents unique challenges that necessitate domain-specific approaches, such as the need to recognize fine-grained hand and finger movements (e.g., fingerspelling) and the grammatical importance of non-manual markers. Among various data modalities, skeleton-based approaches are particularly well-suited for SLR as they provide a detailed representation of the body and hand articulation crucial for linguistic interpretation. The evolution of skeleton-based models for this task often mirrors the advancements in the broader HAR field. Du et al. [12] have proposed a method using a Recurrent Neural Network (RNN) [13] for Skeleton-Based HAR that can appropriately model long-term contextual information in temporal sequences. This addresses limitations in capturing contextual information due to time window size constraints and difficulties in adapting to sequence data inherent in conventional methods using Temporal Pyramids (TPs) [14–16] or Hidden Markov Models (HMMs) [17–19]. Liu et al. [20] have introduced LSTM module with new gating mechanism to deal with the noise in the skeletal data. Liu et al. [21] have also proposed effective Action-Part Semantic Relevance-aware (APSR) framework which incorporates the 2D Spatial-Temporal LSTM (ST-LSTM) [20]. However, the capability of these methods is limited as they do not explicitly exploit the spatial relationships among the joints, which are crucial for understanding human actions.

On the other hands, the emergence of Graph Convolutional Networks (GCNs), which extend Convolutional Neural Networks (CNNs) to non-Euclidean graph structures, enabled the development of the Spatial-Temporal Graph Convolutional Network (ST-GCN) proposed by Yan et al. [2], which effectively captures both spatial dependencies among joints and temporal dynamics. This model marked a major breakthrough in skeleton-based action recognition. Following this breakthrough, various ST-GCN vari-

ants [22–26] emerged. Among them, Inception ST-GCN [25] aimed to capture relationships with more distant joint points and symmetric points. CTR-GC [26] was proposed as a method that improves upon this by utilizing dynamically estimated channel-specific correlations from input data to generate a learnable shared topology, thereby producing distinct adjacency matrices for each channel.

Recently, Multihead Self-Attention mechanism and Transformer have been successful in Natural Language Processing [11] and Computer Vision [27]. Recent studies have focused on the difficulty of capturing long-range dependencies in existing RNN-, CNN-, and GCN-based models, and have proposed approaches that leverage the strength of self-attention mechanisms in modeling such long-range dependencies. Cho et al. [28] have developed the Temporal Segment Self-Attention Network (TS-SAN), a hybrid architecture combining Self-Attention Network (SAN) variants with the Temporal Segment Network (TSN) framework. Plizzari et al. [29] have designed two modules, one is Spatial Self-Attention (SSA) to dynamically model intra-frame interactions and relationships between body parts within a single frame, other is Temporal Self-Attention (TSA) to capture inter-frame correlations and the dynamics of each joint across the entire temporal sequence. Then, they have proposed a two-stream Spatial Temporal Transformer Network (ST-TR) that combines an S-TR stream (SSA + TCN) and a T-TR stream (GCN + TSA) for comprehensive feature extraction. Various Transformer-based variants [30–32] for Skeleton-Based HAR continue to be proposed, with performance improving day by day.

2.3 Sign Language and Fingerspelling Recognition

As mentioned previous subsection, SLR is specialized and challenging sub-domain of HAR. Sign language recognition (SLR) tasks are generally categorized into three main types: ISLR, CSLR, and SLT. ISLR focuses on recognizing individual lexical signs, while CSLR and SLT aim to convert sign sequences into word sequences or natural language sentences, often requiring the integration of natural language processing techniques. Although ISLR deals with isolated

signs, it remains an essential research direction, as it often serves as a foundation or pretraining stage for more complex tasks such as CSLR and SLT [33]. In particular, many skeleton-based studies have primarily targeted the ISLR setting, where clear temporal segmentation allows for detailed modeling of spatial-temporal dynamics in sign gestures. As this study specifically focuses on the ISLR task, we present prior work on ISLR separately from that on fingerspelling recognition, so as to clearly distinguish the methodological developments and challenges in each research area.

2.3.1 Fingerspelling Recognition

Fingerspelling is a kind of sign language, and is the practice of representing the characters of a written language’s alphabet using a set of prescribed handshapes. It serves as an essential tool within sign languages to convey words for which no sign exists, such as proper nouns (e.g., names, places), technical terms, or loanwords. Fingerspelling can be classified from still images because most of its gestures are static. Nicolas Pugeault and Richard Bowden [34] present interactive hand shape recognition user interface for American Sign Language (ASL) fingerspelling using Microsoft Kinect device. After hand detection, a total of 2048-dimensional features are extracted from both the intensity image and depth image using a bank of Gabor filters. Random Forest is employed for classification, distinguishing 24 static target gestures excluding ‘j’ and ‘z’, achieving a reported mean precision of 75%. Subsequently, methods combining feature extraction using Binary Appearance and Shape Elements (BASE) or scale-Invariant Feature Transform (SIFT) with machine learning models such as Support Vector Machine (SVM) [35] or k-Nearest Neighbors (KNN) [36] have been proposed [37–39]. Meanwhile, with the advent of Convolutional Neural Networks, image classification models began to be adopted for fingerspelling tasks as well. Salem Ameen and Sunil Vadera [40] adopted ConvNet [41] to classify the ASL fingerspelling. Unlike conventional methods that employ machine learning classifiers after feature extraction, They adopted a ConvNet architecture that processes depth and intensity (color) information

separately, achieving 82% precision and 80% recall performance. Similarly, Crespo et al. [42] achieved a classification accuracy of 94.8% by fine-tuning a pre-trained VGG19 [43] model for ASL classification using transfer learning and data augmentation techniques. Das et al. [44] also adopted InceptionV3 [45] and reported consistently high accuracy exceeding 90% on the validation set, achieving a maximum accuracy of 98%. Recently, Miah et al. [46] proposed new CNN model, called BenSignNet, consisted of 9 conventional layers and achieved 94.00%, 99.60%, and 99.60% for the BdSL Alphabet [47], KU-BdSL [48], and Ishara-Lipi [49] datasets, respectively.

Simultaneously, pose estimation technology has advanced, leading to an increase in skeleton-based methods. Shin et al. [50] proposed ASL fingerspelling recognition method by utilizing Mediapipe Hands [51] as hand skeleton extractor. They calculated features such as distances between keypoints and joint angles from the extracted keypoint coordinates, and reported recognition accuracies of 99.39% and 98.45% using SVM and light GBM [52]. Recently, multimodal approaches combining RGB and skeleton data have also been proposed. Shin et al. [53] proposed the combined feature extraction method: one is hand-crafted feature was extracted from skeleton data, other was extracted by CNN. Their proposed method was evaluated on Korean Sign alphabet and digit (fingerspelling), arabic fingerspelling and ASL fingerspelling datasets and archived 92.04%, 93.54%, 92.60% and 98.89% classification accuracy, respectively.

2.3.2 Isolated Sign Language Recognition

Moving beyond the character-level task of finger-spelling, word-level Sign Language Recognition (SLR) introduces a significant leap in complexity. First, unlike finger-spelling, which is often articulated with a single hand, most signs are dynamic gestures that involve coordinated movements of both hands, the arms, the torso, and grammatically crucial non-manual markers such as facial expressions. This requires models to process holistic upper-body information rather than focusing on a single limb. Second, the vast majority of signs are inherently dynamic, where the meaning is conveyed through the entire trajectory of the mo-

tion, not by a static pose. This necessitates robust spatio-temporal modeling to capture the subtle evolution of the gesture over time. Finally, the task is compounded by the challenge of scale; a practical SLR system must distinguish between a vast vocabulary, often consisting of hundreds or thousands of unique signs. These factors combined make word-level SLR a highly demanding recognition task, pushing the boundaries of action recognition models.

Huang et al. [54] proposed an early deep learning model for Sign Language Recognition using a 3D Convolutional Neural Network (3D CNN). A key aspect of their work was the use of multi-channel inputs—fusing color, depth, and skeleton data—to automatically learn spatio-temporal features from video. On a self-collected 25-word dataset, their 3D CNN achieved 94.2% accuracy, significantly outperforming a traditional GMM-HMM baseline. Joze et al. [55] also applied the I3D [5] model and evaluated it on new large scale ASL dataset called MS-ASL. They reported that their approach significantly outperformed existing methods such as 2D-CNN+LSTM and skeleton-based methods in recognition accuracy, demonstrating the effectiveness of pre-trained I3D. Li et al. [3] introduced new large-scale ASL dataset called WLASL, and evaluated vision based approach and skeleton based approach. They proposed two vision based approaches (2D CNN + GRU and I3D), and two skeleton based approaches (Pose-RNN and Pose-TGCN). It was confirmed that pre-trained I3D remains an effective vision-based method even for newly proposed datasets. Furthermore, Pose-TGCN demonstrated superiority over simple RNN methods, indicating that its ability to model spatial relationships between body parts in addition to joint point time-series relationships contributed to improved accuracy. However, they also point out that all methods show a significant drop in accuracy when the vocabulary size increases to 2000, highlighting the difficulty of large-scale sign language recognition. Miah et al. [56] proposed multi-stream graph based deep neural network for word-level sign language recognition. They input four pieces of information into a graph-based neural network: keypoints, vectors composed of two keypoints (bones), and the temporal differences between keypoints and bones (joint motion and bone motion).

By concatenating features extracted from each stream to make the final prediction, they achieved 96.45% and 89.45% accuracy on the AUTSL [57] and CSL [3] datasets, respectively. Hu et al. [8, 9, 58] focused on the challenge that limited labeled training data makes models prone to overfitting. Drawing inspiration from BERT—which achieved significant success in natural language processing—and its training methodology, they proposed a self-supervised learning approach and a novel model tailored for sign language recognition. The model they propose captures the shape of the hand and the connections between joints in each frame as a graph structure. It extracts features using a Graph Convolutional Network (GCN) and inputs the sequence of hand movements into a Transformer encoder. This enables the calculation of relationships between all hand poses within the sequence, allowing for the acquisition of context-aware representations. SignBERT archived 79.07%, 70.36% and 47.46% classification accuracy on WLALS100, 300 and 2000, respectively. And SignBERT+ archived 79.84%, 73.20% and 48.85% on same dataset. Liu et al. [6] have proposed a channel-wise Graph Neural Network (GNN) that uses Channel-wise Topology Refinement Graph Convolution (CTR-GC) [7] as its core backbone. They focused on the problem that the density of keypoints on the hands and face is significantly higher than that on the torso, and that models struggle to handle this imbalance. To address this issue, they introduced the Parallel Non-manual And Manual (PANAM) module and the Motion Excited Temporal Re-weighting (METR) module. They also introduced a data augmentation technique based on PartMixing for Skeleton, and by training the proposed model, achieved a classification accuracy of 55.37% on WLALS2000, demonstrating a significant improvement in accuracy. Patra et al. [59] proposed a novel model called the Hierarchical Windowed Graph Attention Network (HWGAT) and further introduced graph attention. Their approach enables the model to partition the human body graph into meaningful subgraphs and apply attention within them, thereby enhancing computational efficiency while enabling focused learning of joint movements critical to sign language gestures. Similarly, it has been confirmed that adding RGB modality further improves classification

accuracy with these methods [3, 8, 9, 58].

Recently, Zuo et al. [60] noted that sign language signs with similar linguistic meanings are also visually very similar. To facilitate model learning for such words, they proposed a method that automatically generates soft labels weighted according to the semantic proximity of the words. Li et al. [61] proposed a method that incorporates LLM into the model to reduce the gap to downstream tasks such as ISLR, CSL, and SLT, demonstrating exceptional performance compared to previous approaches. Despite these successes, while some approaches utilize Transformers to capture context (temporal information), GCNs are employed to capture spatial information. GCN aggregates spatial information based on a predefined fixed structure, which limits its ability to capture relationships between physically separated joints.

In this paper, we propose a Transformer-based approach to maximize the characteristics of Transformers and capture spatio-temporal relationships, addressing the limitations of GCNs.

3 Datasets

There are many sign language datasets publicly available for individual sign languages. This study considered three datasets for ASL, JSL, and KSL. The objective of this study is to demonstrate that the proposed method is not over-optimized for a single task or language. To this end, we intentionally selected datasets with different characteristics. Specifically, we included tasks of different granularities: (1) **word-level sign language** (WLALS) and (2) **character-level fingerspelling** (JSL/KSL). Furthermore, by using data from (3) **different linguistic and cultural backgrounds** (American, Japanese, and Korean), we also evaluate the cultural robustness of our method. Among them, WLALS is a large-scale dataset for ASL. Furthermore, to demonstrate the generality of the proposed method, we also evaluated it on two finger spelling datasets.

Table 1: Evaluated Dataset Description in the Study

| Dataset Name | Lang. | Signs | Sub. | Total Videos | Videos Per Sign | Joints Per Frame |
|--------------|-------------------------|-------|------|--------------|-----------------|------------------|
| WLASL | ASL | 2000 | 119 | 21089 | 10.5 | 67 |
| JSL | Japanese fingerspelling | 46 | 15 | — | — | 21 |
| KSL | Korean fingerspelling | 32 | 20 | — | — | 21 |

3.1 WLASL Dataset

The WLASL dataset is one of the largest video resources for word-level American Sign Language (ASL) recognition, containing 68,129 videos featuring 20,863 unique ASL glosses collected from 20 diverse websites [3]. Each video captures a signer performing a single sign, typically from a frontal view, with varying background complexities. This dataset aims to advance research in sign language recognition and improve communication between deaf and hearing communities. To maintain consistency, gloss annotations with more than two English words were excluded, and glosses with fewer than seven video samples were removed to ensure adequate data for training and testing. After preprocessing, the dataset comprises 34,404 videos for 3,126 glosses, organized by sample count. WLASL is divided into four subsets based on vocabulary size: WLASL100, WLASL300, WLASL1000, and WLASL2000, representing the top 100, 300, 1,000, and 2,000 glosses, respectively. These subsets enable the evaluation of word-level recognition challenges across different vocabulary sizes. The dataset also supports scalability testing for sign recognition methods. WLASL remains an essential resource for developing innovative, large-scale sign language recognition systems.

3.2 Japanese Sign Language (finger-spelling) Dataset

Japanese Sign Language (JSL) datasets are limited, particularly for dynamic signs. A new JSL dataset was created using an RGB camera to address this gap, capturing both static and dynamic signs. This dataset comprises (76 kinds of Japanese fingerspelling \times 15 signers =) 1140 videos collected from 15 non-

native signer aged 18 to 25. Each participant recorded one video for each of the 76 JSL alphabet signs (46 static and 30 dynamic), ensuring diverse representation. The data collection process followed a structured approach. Participants were seated before the camera and instructed to observe a finger-spelling model before mimicking the signs. Recording one character took approximately 1 seconds, with each participant spending about 10 minutes to complete all 76 signs. Static signs have consistent data representation, while dynamic signs show variability in time and data volume, depending on individual performance. The dataset provides valuable resources for studying static and dynamic JSL recognition, addressing a key challenge in developing comprehensive sign language models. It offers detailed insights into the variability of dynamic gestures while maintaining consistency for static gestures. Figures and tables associated with the dataset offer further context, showcasing examples of signs and highlighting the differences between static and dynamic gestures. This dataset is a significant step toward advancing JSL recognition research.

3.3 Korean Sign Language (finger-spelling) dataset

We also used the Korean Sign Language (finger-spelling) dataset was collected in previous our lab's work, and it has 31 kinds of fingerspelling gestures. This dataset has 620 videos were recorded by 20 non-native signers. Each video's duration is approximately 3 seconds. In this experiment, we extracted 21 hands keypoints by Mediapipe from each frame.

Figure1 shows the skeleton structure for JSL and KSL as input data.

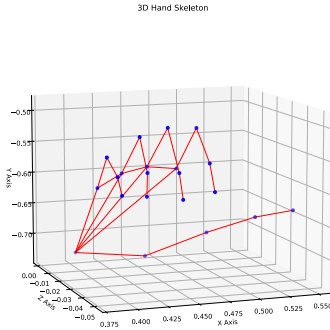


Figure 1: Skeleton graph for FignerSpelling.

4 Proposed Methodology

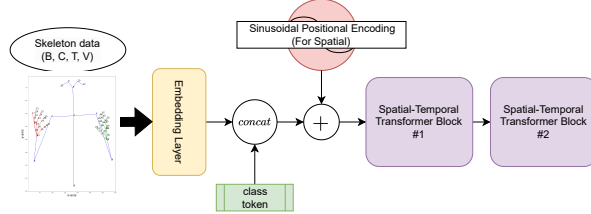


Figure 2: The overview of proposed architecture.

Figure 2 represents the structure of the proposed architecture based on the transformer. Transformers have been used as deep learning methods for a variety of tasks (e.g., *Natural Language Processing*, and *Computer Vision*), and have demonstrated great performance and their effectiveness. One of advantages in Transformer is allowing to capture the relationship between long-term in early stage. Another approach used in skeleton-based human action recognition and hand gesture recognition is the graph-convolution network, which uses a graph to convolve adjacent nodes. This approach can capture the relationship between adjacent nodes, but it requires multiple convolution layers to capture the relationship between non-adjacent nodes. For these reasons, we employed the Transformer in our approach.

This diagram 3 illustrates the structure of the

skeleton input into our proposed method. Since our method is composed of Transformers, there is no need to predefine the skeleton structure as a graph, as is required with GCNs.

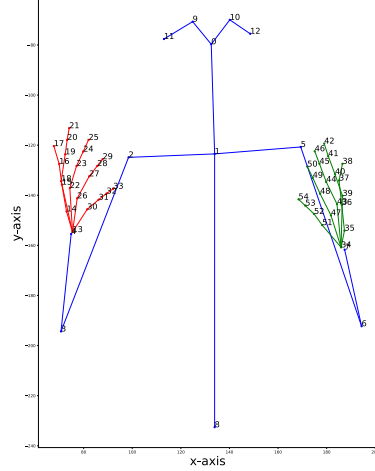


Figure 3: Pose and graph construction for WLASL.

The skeleton data as input data fed into embedding layer which changes coordinates into embedding vectors. Then, the embedding vectors were concatenated with *class token*, added with Sinusoidal Positional Encoding, and passed multiple spatial temporal transformer blocks. In the transformer block, embedding data was applied spatial self-attention, temporal self-attention, and feed forward network. After that, the *class token* was extracted and fed into the fully connected layer. Finally, we obtained the predicted label. In the following subsections, each component of the proposed method is explained.

4.1 Spatial Temporal Transformer Block

Figure 4 shows the internal structure of Spatial Temporal Transformer Block. The design of this block was inspired by previous work in the field of action recognition [2], which demonstrated the effectiveness of a sequential spatial-then-temporal architecture. We adopted this design, positing that sequentially processing spatial and temporal features would be simi-

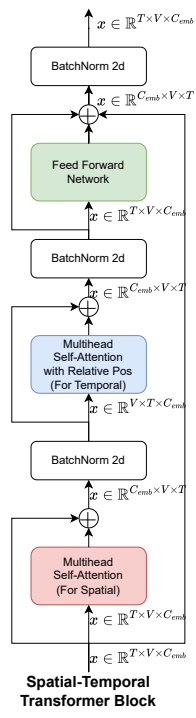


Figure 4: The internal structure of Spatial Temporal Transformer Block.

larly effective for the sign language recognition task. This block mainly consisted of 3 components : Multihead Self-Attention for spatial dimension, Multihead Self-Attention for temporal dimension with Relative Positional Encoding, and Feed Forward Network. The position of the normalization layer in the Transformer is often discussed, and there are two types: Post-Norm, which places the normalization layer between residual blocks, and Pre-Norm, which places it inside the residual connection and places it before Self-attention. In our architecture, we adopted the Post-Norm structure because Post-Norm performs better for relatively shallow transformers [62], and we also observed that Post-Norm performs better than Pre-Norm in this experiment. However, when Post-Norm is multi-layered, learning tends to become unstable. Recently, a method called B2T Connection [63], which skips all sub-layers, has been proposed to solve this problem, and it has been successful in multi-layering Post-Norm. So, we used this technique for stabilizing the model learning.

4.2 Multihead Self-Attention For Spatial dimension

The input embedding vectors first met multihead self attention for spatial dimension. Figure 5 shows the structure of multihead self attention for spatial dimension. Let denote the input embedding vectors as $x \in \mathbb{R}^{T \times V \times C_{emb}}$. T represents the length of the sequence, V represents the number of vertices or nodes, and C_{emb} represents the number of embedding channels. Input embedding vectors fed into each linear layer to product *query*, *key*, and *value*. These process are expressed as follows:

$$query = W_q(x) \quad (1)$$

$$key = W_k(x) \quad (2)$$

$$value = W_v(x) \quad (3)$$

Then, the attention map was calculated by the dot product operation with *query* and *key*. Finally, the output of attention was computed by *matmul* operator with attention map and *value*, and projected by output's linear layer as follows:

$$output = W_o(MatMul(attention, v)) \quad (4)$$

As mentioned above, Graph Convolution can generally capture the relationships between adjacent nodes, but cannot capture the relationships between non-adjacent nodes. On the other hand, by using Self-Attention, each node can access all nodes, and it plays a role in capturing the relationships between nodes at an early stage.

4.3 Multihead Self-Attention with Relative Positional Encoding for Temporal dimension

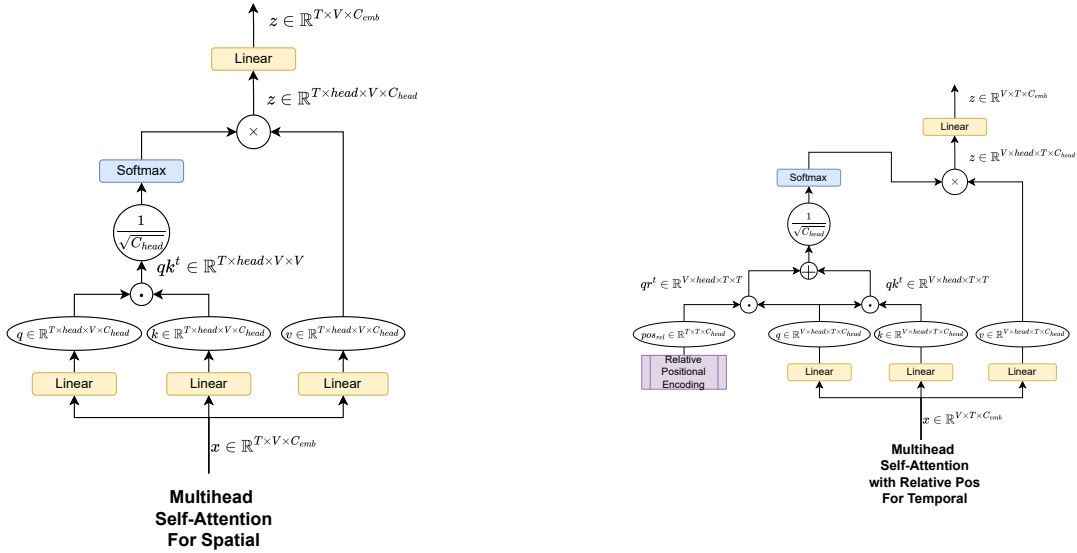


Figure 5: Multihead Self Attention for spatial dimension.

Figure 6: Multihead Self Attention with Relative Positional Encoding for temporal dimension.

Figure 6 shows the structure of Multihead Self Attention with Relative Positional Encoding. This component aims to capture the relationships between different frames along a temporal dimension. However, this component does not use relative position encoding along the temporal dimension. This module is inspired by [64], and gets a temporal translation invariance that maintains robust performance even if a particular frame is moved forward or backward. In our model, the input embedding vector was transposed in spatial and temporal dimensions before being passed to this module.

4.4 Feed Forward Network

Following the general transformer architecture, the embedding vectors which went through the attention module, fed into the feed forward network that has two linear projection layers and one activation function. More specifically, the input vector is expanded to a dimension 4.0 times larger than the embedding dimension by a first linear projection layer (as defined by the FFN Expand Ratio in Table 2), then nonlinearly transformed via an GELU [65] activation function, and then converted back to a lower dimension by another linear projection layer, where the vector is merged by addition. This process is expressed as follows:

$$x_{ffn} = GELU(W_1(x)) \quad (5)$$

$$x = W_2(x_{ffn}) + x \quad (6)$$

4.5 Data Augmentation for Skeleton Data

In deep learning, the amount of data is one of the important aspects in obtaining a better learning representation. If training is done with insufficient data, the deep learning model tends to overfit. However, due to high annotation cost, current labeled sign data sources are limited. To tackle this issue, some works adopted data augmentation [66] technique, or the self-supervised learning approach [8,9,58] in Sign Language Recognition task.

In this experiment, we also adopted some data augmentation techniques to avoid the overfitting. As basic augmentation technique, we applied random rotation and random shifting to xy skeleton coordinates data. The rotation range is between -15 degrees and 15 degrees, and the shift ranges from -0.1 to 0.1, with changes applied to the x and y axes separately. These process is expressed as follows:

$$\tilde{x} = (x \cos \theta - y \sin \theta) + \Delta x \quad (7)$$

$$\tilde{y} = (x \sin \theta + y \cos \theta) + \Delta y \quad (8)$$

Δx and Δy denote as shifting value, and θ denote as rotation degrees.

In addition, we also adopted the Joint Mixing Data Augmentation [67] which can generally improve the effectiveness and robustness.

To handle video inputs of varying lengths and to augment the training data, we employed different frame sampling strategies for the training and inference phases. **For training**, we used a random temporal sampling strategy. From a given video sequence V with a total of T frames, we randomly selected a starting frame and extracted a continuous clip of a fixed length L . If the video is shorter than the desired length ($T \leq L$), we padded the sequence by repeating the last frame until it reaches the length L . This acts as a form of data augmentation, ensuring the model sees different segments of the video in each epoch, which improves its robustness. **For validation and testing**, we adopted a uniform sampling strategy to ensure a comprehensive and deterministic evaluation. We extracted k evenly-spaced, overlapping clips of length L from the entire video sequence. The starting frame index s_i for the i -th clip (where $i \in \{0, 1, \dots, k-1\}$) is determined as:

$$s_i = \lfloor i \times \frac{T-L}{k-1} \rfloor + 1$$

The final prediction for the video was obtained by averaging the softmax prediction scores from all k clips. This multi-view inference approach provides a more stable and reliable assessment of the model's performance. In our experiments, we set the clip length L to 50 frames for WLASL dataset, and 32 frames for JSL and KSL, and the number of clips k to 4 for all datasets.

4.6 Experimental Setting

The JSL and KSL dataset was split into training, validation, and testing sets using a 8:1:1 ratio, ensuring each gloss had at least one sample in both splits, and keeping user-independent condition that means the each set does not contain data come from the same user. In other words, each dataset consists of data from different users only, ensuring that no single user's data appears in multiple sets. This condition is crucial for evaluating a model's generalization performance, as it prevents overfitting to specific users and allows

for a more accurate assessment of how the model performs on unseen data. For WLASL dataset, we evaluated the performance with following the official splitting which is provided by json file.

All experiments were conducted on a machine equipped with a GeForce RTX 5090 GPU (32GB VRAM), 32GB RAM, and CUDA 12.8.1. Our implementation is based on PyTorch [68].

We based our training configuration on a set of standard hyperparameters commonly used in the Transformer and skeleton-based recognition literature, ensuring a robust and reproducible baseline [69]. Models were trained from scratch using the **AdamW optimizer** [70], a standard choice for Transformer models. To ensure stable training, we employed a **cosine annealing scheduler** with a linear warmup of 5 epochs. The base learning rate was set to 1.0×10^{-3} , a typical and effective starting point for this architecture when paired with AdamW.

The per-device batch size was set to 16, which was the maximum size that could be accommodated by our GPU memory (GeForce RTX 5090, 32GB VRAM). To achieve a larger and more stable effective batch size, we employed **gradient accumulation for 16 steps**, resulting in an effective batch size of 256.

Unlike large-scale pre-training on datasets like ImageNet, which often converge in fewer epochs, training Transformer models from scratch on **small-to-medium-sized datasets** like WLASL, JSL, and KSL requires a significantly longer training duration to achieve convergence while avoiding overfitting. Therefore, we trained models for **1500 epochs on WLASL** and **1000 epochs on JSL and KSL**. This extended duration was intentionally set to allow the cosine annealing scheduler to fully complete its cycle, ensuring the model could learn robust representations and converge properly from these limited datasets.

For regularization and training stability—common challenges in deep Transformer models, especially on smaller data—we applied a standard set of techniques: **label smoothing** (0.05), **gradient clipping** (10.0), **FFN dropout** (0.25), and **Stochastic Depth** (0.25).

The detailed model architecture specifications and all training hyperparameters are summarized in Table 2. The output layer’s neurons were matched to the number of classes for each dataset (e.g., 100 for

WLASL100, 46 for JSL, and 32 for KSL). The specific frame sampling strategies for training and testing are detailed in Section 4.5. To ensure a robust evaluation of our model’s stability, we did not use a single fixed seed. Instead, we conducted all experiments 10 times, using 10 different random seeds (integers 0 through 9). The results presented in tables (e.g., Table 5) report the mean, standard deviation, and best performance across these 10 runs.

Table 2: Key hyperparameters for our experiments.

| Parameter | Value |
|-------------------------------|--------------|
| Model Architecture | |
| Embedding Dimension | 128 |
| Number of Blocks | 10 |
| Number of Heads | 8 |
| Head Dimension | 64 |
| FFN Expand Ratio | 4.0 |
| Data & Training | |
| Epochs | 1500 |
| Batch Size | 16 |
| Accumulation Steps | 16 |
| (Effective Batch Size) | (256) |
| Input Sequence Length (L) | 50 |
| Number of Joints | 55 |
| Test Clips (k) | 4 |
| Optimization (AdamW) | |
| Base Learning Rate | 0.001 |
| Weight Decay | 0.01 |
| Betas | (0.9, 0.999) |
| Epsilon | 1.0e-08 |
| LR Scheduler | Cosine |
| Warmup Epochs | 5 |
| Warmup Init LR | 0.0001 |
| Minimum LR | 1.0e-05 |
| Regularization | |
| Label Smoothing | 0.05 |
| Gradient Clip Norm | 10.0 |
| FFN Dropout | 0.25 |
| Stochastic Depth Rate | 0.25 |

4.7 Evaluation Metrics

For evaluation, we reported the classification accuracy following [3], *i.e.*, Top-1 (**T-1**) and Top-5 (**T-5**) per instance for WLASL dataset, and presented the Top-1 classification accuracy on JSL and KSL dataset. Top-K accuracy represents the proportion of samples where the correct label appears among the model’s top-K predicted classes. The performance of deep learning models is often sensitive to stochastic elements, including weight initialization and data shuffling order. A single training run may therefore not be representative of the model’s true capability. To ensure a fair and robust evaluation and to enhance the reproducibility of our results, we repeated every experiment 10 times, each with a unique random seed. In our result tables, we present the mean accuracy as the primary metric, accompanied by the standard deviation (std) to indicate the stability of the model, and the maximum (max) accuracy to show its peak potential.

5 Experimental Results

In the study, we used various experiments with sign language and fingerspelling dataset including ASL, JSL, and KSL, to demonstrate the superiority and effectiveness of the proposed model.

5.1 State of the art similar work comparison for the JSL Dataset

The state-of-the-art comparison of the proposed model’s performance against existing methods is presented in Table 3. The results demonstrate that the proposed model outperforms existing approaches in Japanese Sign Language (JSL) recognition. Among the existing methods, Ikuno et al. utilized a smartphone camera to collect JSL data, employing MediaPipe to extract hand skeleton features based on distance metrics. They classified gestures using a random forest algorithm, achieving 70–80% accuracy [71]. Kwolek et al. proposed a three-step approach for JSL alphabet recognition, beginning with a 3D articulated hand model and synthetic data generation using a

GAN. They then applied ResNet34 for segmentation and used an ensemble model for classification, achieving 92.1% accuracy [72]. Kobayashi et al. grouped visually similar dynamic signs, such as \textcircled{N} (no) and \textcircled{Y} (ri), into subclasses to improve classification. Using OpenPose for skeleton extraction and MSVM for classification, they achieved 96% accuracy [73]. The proposed Transformer-based model achieved a 99.34% accuracy as best performance, surpassing most existing methods for both static and dynamic signs. This highlights its superior capability in JSL recognition tasks.

5.2 Performance Accuracy and State of the Art Comparison of the KSL Dataset

Table 4 provides a performance comparison of various models on the New KSL dataset for sign language recognition. The existing work [75] adopted two-stream feature extraction approach: hand-crafted feature and extracted feature from pretrained image classification model, and used SVM [35] for classifying the Korean fingerspelling. They reported the 92.04 % classification accuracy at the time. On the other hand, our proposed Stack Transformer achieves the performance accuracy at 95.16% as best performance. As a matter of fact, KSL dataset consisted of static fingerspelling only. Most of case, fingerspelling can be predicted by single frame. So, this comparison might be not fair because our proposed model requires the sequence of skeleton data for handling both static and static gesture. However, proposed model has also been shown to be effective against static fingerspelling.

5.3 Performance Accuracy and State of the Art Comparison of the WLASL Dataset

Table 6 provides a comprehensive comparison of state-of-the-art skeleton-only methods on the WLASL dataset across multiple configurations. Below, we briefly review the key approaches before presenting our results.

Table 3: State of the art-similar work comparison of the proposed model with JSL Dataset

| Method | Algorithm | Type of Sign | Test Best Accuracy (Mean \pm Std) [%] |
|------------------------|--------------------|-------------------------|--|
| Ikuno et al. [71] | Random Forest | Static | 79.20 |
| Kwolak et al. [72] | Deep CNN | Static | 92.10 |
| Kobayashi et al. [73] | SVM | Static / Dynamic | 65.00 / 96.00 |
| Kakizaki et al. [74] | SVM | Static + Dynamic | 97.20 |
| Proposed method | Transformer | Static + Dynamic | 99.34 (94.80 \pm 2.87) |

Table 4: State-of-the-art comparison for the new KSL dataset.

| Method | Modality | Type of Sign | Test Best Accuracy (Mean \pm Std) [%] |
|------------------------|-------------------------------|---------------|--|
| Shin et al. [75] | Skeleton (single frame) | Static | 92.04 |
| Proposed method | Skeleton (multi-frame) | Static | 95.16 (84.60 \pm 10.44) |

Table 5: Detailed performance and robustness evaluation of our model on all subsets of the WLASL dataset (WLASL100, and WLASL300). We report per-instance and per-class Top-1 and Top-5 accuracy (%) for each of the 10 runs with different random seeds. The mean, standard deviation (std.), and best results are summarized at the bottom.

| Run (Seed) | WLASL100 | | | | WLASL300 | | | |
|-----------------|------------------|------------------|------------------|------------------|------------------|------------------|------------------|------------------|
| | Per-Instance (%) | | Per-Class (%) | | Per-Instance (%) | | Per-Class (%) | |
| | Top-1 | Top-5 | Top-1 | Top-5 | Top-1 | Top-5 | Top-1 | Top-5 |
| Seed 0 | 79.46 | 92.64 | 80.80 | 93.42 | 74.10 | 92.51 | 75.01 | 92.89 |
| Seed 1 | 82.56 | 93.41 | 83.47 | 94.25 | 73.65 | 92.66 | 74.33 | 92.89 |
| Seed 2 | 82.17 | 93.41 | 83.22 | 94.17 | 74.85 | 92.81 | 75.56 | 93.17 |
| Seed 3 | 82.17 | 94.96 | 83.22 | 95.75 | 73.80 | 93.11 | 74.45 | 93.39 |
| Seed 4 | 80.62 | 94.96 | 81.88 | 95.88 | 72.75 | 92.51 | 73.71 | 92.78 |
| Seed 5 | 81.78 | 94.57 | 82.80 | 95.42 | 74.55 | 92.07 | 75.41 | 92.39 |
| Seed 6 | 82.95 | 95.35 | 84.55 | 95.92 | 73.35 | 92.07 | 74.02 | 92.61 |
| Seed 7 | 80.62 | 93.02 | 81.97 | 94.00 | 73.05 | 92.81 | 73.91 | 93.10 |
| Seed 8 | 80.62 | 93.80 | 81.30 | 94.58 | 74.70 | 91.92 | 75.63 | 92.39 |
| Seed 9 | 82.95 | 93.41 | 84.38 | 94.08 | 72.31 | 92.07 | 73.11 | 92.33 |
| Mean \pm Std. | 81.59 \pm 1.19 | 93.95 \pm 0.93 | 82.76 \pm 1.25 | 94.75 \pm 0.91 | 73.71 \pm 0.86 | 92.45 \pm 0.40 | 74.51 \pm 0.86 | 92.79 \pm 0.00 |
| Best | 82.95 | 95.35 | 84.55 | 95.92 | 74.85 | 93.11 | 75.63 | 93.39 |

Table 6: State-of-the-art comparison for **skeleton-only** methods on the WLASL Dataset. Modality is abbreviated as: S (skeleton), H (hands), P (full keypoints), and RGB (RGB frames). All our results report the best Per-Instance accuracy achieved across 10 runs, with the mean and standard deviation shown in parentheses.

| Method | Modality | WLASL100 | | WLASL300 | | WLASL1000 | | WLASL2000 | |
|------------------------|----------|------------------|------------------|------------------|------------------|-----------|-------|-----------|-------|
| | | Top-1 | Top-5 | Top-1 | Top-5 | Top-1 | Top-5 | Top-1 | Top-5 |
| Pose-GRU [3] | S | 46.51 | 76.74 | 33.68 | 64.37 | 30.01 | 58.42 | 22.54 | 49.81 |
| Pose-TGCN [3] | S | 55.43 | 78.68 | 38.32 | 67.51 | 34.86 | 61.73 | 23.65 | 51.75 |
| GCAR [76] | S | 63.25 | 80.00 | 43.80 | 69.01 | — | — | 24.10 | 52.62 |
| Sign2Pose [77] | S | 80.9 | — | 64.21 | — | 49.46 | — | 38.65 | — |
| SignBERT [8] | S (H) | 76.36 | 91.09 | 62.72 | 85.18 | — | — | 39.40 | 73.35 |
| SignBERT [8] | S (H+P) | 79.07 | 93.80 | 70.36 | 88.92 | — | — | 47.46 | 83.32 |
| SignBERT+ [9] | S | 79.84 | 92.64 | 73.20 | 90.42 | — | — | 48.85 | 82.48 |
| BEST [58] | S | 77.91 | 91.47 | 67.66 | 89.22 | — | — | 46.25 | 83.32 |
| SKIM [6] | S | 74.42 | 90.72 | 73.95 | 92.67 | — | — | 55.37 | 86.98 |
| Ours (Mean \pm Std.) | S | 81.59 ± 1.19 | 93.95 ± 0.93 | 73.71 ± 0.86 | 92.45 ± 0.40 | — | — | — | — |
| Ours (Best) | S | 82.95 | 95.35 | 74.85 | 93.11 | — | — | — | — |

The authors of the WLASL dataset [3] provided two baseline models, Pose-GRU (46.51% Top-1 on WLASL100) and the GCN-based Pose-TGCN (55.43%). More recent methods have achieved significant gains by employing self-supervised learning (SSL). Approaches like SignBERT [8], SignBERT+ [9], and BEST [58], inspired by the BERT large language model, first learn general representations via pre-training and are then fine-tuned on downstream tasks. Among these, SignBERT+ [9] established the previous state-of-the-art for skeleton-only methods with 79.84% on WLASL100. Other works, such as SKIM [6], adopted novel backbones (CTR-GCN) and data augmentation (Part Mixing), demonstrating strong performance, especially on the large-scale WLASL2000 subset (55.37%).

In our work, our proposed model achieves a new state-of-the-art performance, with a best Top-1 accuracy of 82.95% on WLASL100 and 74.85% on WLASL300. This result is particularly significant because our model, trained entirely from scratch, demonstrates superior performance over previous state-of-the-art methods that leverage self-supervised learning frameworks.

We acknowledge that multi-modal methods, such as SignBERT+ (S + **RGB**) [9], which leverage rich

visual information from RGB frames, can achieve a higher absolute accuracy. However, our work focuses on the skeleton-only domain, which is crucial for applications requiring computational efficiency, privacy preservation, and robustness to background noise. In this challenging and practical category, our from-scratch method establishes a new state-of-the-art. This strong performance suggests that our model acquires sufficient expressive power from limited data, indicating potential for further improvement through the future application of self-supervised pre-training.

6 Discussion

In our experiments, the proposed model was evaluated on three distinct datasets: the Japanese Sign Language (JSL) and Korean Sign Language (KSL) fingerspelling datasets, and the large-scale word-level WLASL dataset.

On both fingerspelling datasets (JSL and KSL), our model achieved state-of-the-art accuracy, outperforming previous methods in classifying both static and dynamic gestures (Tables 3 and 4). We attribute this strong performance on fingerspelling to the Transformer’s ability to capture subtle, high-frequency tem-

poral changes between static poses, a task where GCN-based models may struggle.

On the large-scale WLASL dataset, as shown in Table 6, our model establishes a new state-of-the-art for skeleton-only methods that are trained from scratch. Notably, our model’s performance is highly competitive with, or even surpasses, several methods that rely on complex self-supervised learning (SSL) to acquire good initial weights.

This strong from-scratch performance is a key finding, suggesting that our sequential spatial-temporal attention mechanism is highly data-efficient and capable of acquiring expressive representations directly from limited data, without relying on large-scale pre-training. Furthermore, it indicates significant potential for further performance improvement if SSL pre-training were to be applied in future work.

Finally, we acknowledge that the highest-performing methods in Table 6 are multi-modal, typically fusing skeleton data with an RGB stream. This highlights a clear limitation of any single-modality approach, including our own. However, it also presents a promising avenue for future enhancement by integrating a visual stream into our powerful Transformer framework.

7 Conclusion

In this paper, we proposed a novel Stacked Spatial-Temporal Transformer Network for Sign Language Recognition (SLR). Our contributions are threefold: First, our model employs a hierarchical, stacked architecture where sequential transformers effectively model both short-range and long-range dependencies. Second, we leverage dual multi-head attention mechanisms—Spatial MHA (intra-frame) and Temporal MHA (inter-frame)—to effectively capture the complex spatio-temporal dynamics inherent in sign language gestures.

We validated our model through extensive experiments on diverse datasets, including JSL, KSL, and WLASL. A key finding of our work is that our model, **trained entirely from scratch**, achieves state-of-the-art performance in the challenging fingerspelling categories and establishes a new SOTA for skeleton-

only methods on WLASL, outperforming several approaches that rely on complex self-supervised pre-training.

As discussed, we believe this strong baseline performance indicates significant potential for further enhancement. For future work, we plan to explore two primary directions: 1) adopting an SSL approach to leverage our model’s data-efficient architecture for even greater performance, and 2) integrating multi-modal data, such as RGB streams. Furthermore, we aim to investigate the integration of Large Vision and Language Models to develop next-generation, highly accurate sign language recognition systems.

ABBREVIATIONS

| | |
|------|--|
| GCN | Graph Convolutional Network |
| GCAR | Graph convolution with attention and residual connection |
| SLR | Sign Language Recognition |
| ASL | American Sign Language |
| RNN | Recurrent Neural Network |
| LSTM | Long short term memory |
| TGCN | Temporal graph convolutional network |
| ML | Machine learning |
| DL | Deep learning |

References

[1] World Health Organization, “Deafness and hearing loss,” <https://www.who.int/news-room/fact-sheets/detail/deafness-and-hearing-loss>, Aug. 2024, accessed: 2025-10-04.

[2] S. Yan, Y. Xiong, and D. Lin, “Spatial temporal graph convolutional networks for skeleton-based action recognition,” in *Proceedings of the AAAI conference on artificial intelligence*, vol. 32, no. 1, 2018.

[3] D. Li, C. Rodriguez, X. Yu, and H. Li, “Word-level deep sign language recognition from video: A new large-scale dataset and methods comparison,” in *Proceedings of the IEEE/CVF winter conference on applications of computer vision*, 2020, pp. 1459–1469.

[4] K. Cho, B. Van Merriënboer, C. Gulcehre, D. Bahdanau, F. Bougares, H. Schwenk, and Y. Bengio, “Learning phrase representations using rnn encoder-decoder for statistical machine translation,” *arXiv preprint arXiv:1406.1078*, 2014.

[5] J. Carreira and A. Zisserman, “Quo vadis, action recognition? a new model and the kinetics dataset,” in *proceedings of the IEEE Conference on Computer Vision and Pattern Recognition*, 2017, pp. 6299–6308.

[6] K. Lin, X. Wang, L. Zhu, B. Zhang, and Y. Yang, “Skim: Skeleton-based isolated sign language recognition with part mixing,” *IEEE Transactions on Multimedia*, vol. 26, pp. 4271–4280, 2024.

[7] Y. Chen, Z. Zhang, C. Yuan, B. Li, Y. Deng, and W. Hu, “Channel-wise topology refinement graph convolution for skeleton-based action recognition,” in *Proceedings of the IEEE/CVF international conference on computer vision*, 2021, pp. 13359–13368.

[8] H. Hu, W. Zhao, W. Zhou, Y. Wang, and H. Li, “SignBERT: Pre-Training of Hand-Model-Aware Representation for Sign Language Recognition ,” in *2021 IEEE/CVF International Conference on Computer Vision (ICCV)*. Los Alamitos, CA, USA: IEEE Computer Society, Oct. 2021, pp. 11067–11076. [Online]. Available: <https://doi.ieeecomputersociety.org/10.1109/ICCV48922.2021.01090>

[9] H. Hu, W. Zhao, W. Zhou, and H. Li, “SignBERT+: Hand-Model-Aware Self-Supervised Pre-Training for Sign Language Understanding ,” *IEEE Transactions on Pattern Analysis & Machine Intelligence*, vol. 45, no. 09, pp. 11221–11239, Sep. 2023. [Online]. Available: <https://doi.ieeecomputersociety.org/10.1109/TPAMI.2023.3269220>

[10] J. Devlin, M.-W. Chang, K. Lee, and K. Toutanova, “Bert: Pre-training of deep bidirectional transformers for language understanding,” in *Proceedings of the 2019 conference of the North American chapter of the association for computational linguistics: human language technologies*, volume 1 (long and short papers), 2019, pp. 4171–4186.

[11] A. Vaswani, N. Shazeer, N. Parmar, J. Uszkoreit, L. Jones, A. N. Gomez, Ł. Kaiser, and I. Polosukhin, “Attention is all you need,” *Advances in neural information processing systems*, vol. 30, 2017.

[12] Y. Du, W. Wang, and L. Wang, “Hierarchical recurrent neural network for skeleton based action recognition,” in *2015 IEEE Conference on Computer Vision and Pattern Recognition (CVPR)*, 2015, pp. 1110–1118.

[13] K. Kawakami, “Supervised sequence labelling with recurrent neural networks,” Ph.D. dissertation, Ph. D. thesis, 2008.

[14] J. Luo, W. Wang, and H. Qi, “Group sparsity and geometry constrained dictionary learning for action recognition from depth maps,” in *2013 IEEE International Conference on Computer Vision*, 2013, pp. 1809–1816.

[15] R. Vemulapalli, F. Arrate, and R. Chellappa, “Human action recognition by representing 3d

skeletons as points in a lie group,” in *2014 IEEE Conference on Computer Vision and Pattern Recognition*, 2014, pp. 588–595.

[16] J. Wang, Z. Liu, Y. Wu, and J. Yuan, “Mining actionlet ensemble for action recognition with depth cameras,” in *2012 IEEE conference on computer vision and pattern recognition*. IEEE, 2012, pp. 1290–1297.

[17] F. Lv and R. Nevatia, “Recognition and segmentation of 3-d human action using hmm and multi-class adaboost,” in *European conference on computer vision*. Springer, 2006, pp. 359–372.

[18] D. Wu and L. Shao, “Leveraging hierarchical parametric networks for skeletal joints based action segmentation and recognition,” in *2014 IEEE Conference on Computer Vision and Pattern Recognition*, 2014, pp. 724–731.

[19] L. Xia, C.-C. Chen, and J. K. Aggarwal, “View invariant human action recognition using histograms of 3d joints,” in *2012 IEEE Computer Society Conference on Computer Vision and Pattern Recognition Workshops*, 2012, pp. 20–27.

[20] J. Liu, A. Shahroudy, D. Xu, A. C. Kot, and G. Wang, “Skeleton-based action recognition using spatio-temporal lstm network with trust gates,” *IEEE Transactions on Pattern Analysis and Machine Intelligence*, vol. 40, no. 12, pp. 3007–3021, 2018.

[21] J. Liu, A. Shahroudy, M. Perez, G. Wang, L.-Y. Duan, and A. C. Kot, “Ntu rgb+d 120: A large-scale benchmark for 3d human activity understanding,” *IEEE Transactions on Pattern Analysis and Machine Intelligence*, vol. 42, no. 10, pp. 2684–2701, 2020.

[22] M. Li, S. Chen, X. Chen, Y. Zhang, Y. Wang, and Q. Tian, “Actional-structural graph convolutional networks for skeleton-based action recognition,” in *2019 IEEE/CVF Conference on Computer Vision and Pattern Recognition (CVPR)*, 2019, pp. 3590–3598.

[23] L. Shi, Y. Zhang, J. Cheng, and H. Lu, “Two-stream adaptive graph convolutional networks for skeleton-based action recognition,” in *Proceedings of the IEEE/CVF Conference on Computer Vision and Pattern Recognition (CVPR)*, June 2019.

[24] Z. Liu, H. Zhang, Z. Chen, Z. Wang, and W. Ouyang, “Disentangling and unifying graph convolutions for skeleton-based action recognition,” in *Proceedings of the IEEE/CVF Conference on Computer Vision and Pattern Recognition (CVPR)*, June 2020.

[25] M. Jiang, J. Dong, D. Ma, J. Sun, J. He, and L. Lang, “Inception spatial temporal graph convolutional networks for skeleton-based action recognition,” in *2022 International Symposium on Control Engineering and Robotics (ISCER)*, 2022, pp. 208–213.

[26] Y. Chen, Z. Zhang, C. Yuan, B. Li, Y. Deng, and W. Hu, “Channel-wise topology refinement graph convolution for skeleton-based action recognition,” in *Proceedings of the IEEE/CVF International Conference on Computer Vision (ICCV)*, October 2021, pp. 13 359–13 368.

[27] A. Dosovitskiy, L. Beyer, A. Kolesnikov, D. Weissenborn, X. Zhai, T. Unterthiner, M. Dehghani, M. Minderer, G. Heigold, S. Gelly et al., “An image is worth 16x16 words: Transformers for image recognition at scale,” *arXiv preprint arXiv:2010.11929*, 2020.

[28] S. Cho, M. Maqbool, F. Liu, and H. Foroosh, “Self-attention network for skeleton-based human action recognition,” in *Proceedings of the IEEE/CVF winter conference on applications of computer vision*, 2020, pp. 635–644.

[29] C. Plizzari, M. Cannici, and M. Matteucci, “Spatial temporal transformer network for skeleton-based action recognition,” in *International conference on pattern recognition*. Springer, 2021, pp. 694–701.

[30] C. Zheng, S. Zhu, M. Mendieta, T. Yang, C. Chen, and Z. Ding, “3d human pose estimation with spatial and temporal transformers,” in *Proceedings of the IEEE/CVF International Conference on Computer Vision (ICCV)*, October 2021, pp. 11 656–11 665.

[31] Y. Zhou, Z.-Q. Cheng, C. Li, Y. Fang, Y. Geng, X. Xie, and M. Keuper, “Hypergraph transformer for skeleton-based action recognition,” *arXiv preprint arXiv:2211.09590*, 2022.

[32] Q. Zhao, C. Zheng, M. Liu, P. Wang, and C. Chen, “Poseformerv2: Exploring frequency domain for efficient and robust 3d human pose estimation,” in *Proceedings of the IEEE/CVF Conference on Computer Vision and Pattern Recognition (CVPR)*, June 2023, pp. 8877–8886.

[33] R. Zuo, F. Wei, and B. Mak, “Towards online continuous sign language recognition and translation,” in *EMNLP*, 2024.

[34] N. Pugeault and R. Bowden, “Spelling it out: Real-time asl fingerspelling recognition,” in *2011 IEEE International Conference on Computer Vision Workshops (ICCV Workshops)*, 2011, pp. 1114–1119.

[35] W. S. Noble, “What is a support vector machine?” *Nature biotechnology*, vol. 24, no. 12, pp. 1565–1567, 2006.

[36] T. Cover and P. Hart, “Nearest neighbor pattern classification,” *IEEE Transactions on Information Theory*, vol. 13, no. 1, pp. 21–27, 1967.

[37] B. Estrela, G. Cámar-Chávez, M. Campos, W. R. Schwartz, and E. R. Nascimento, “Sign language recognition using partial least squares and rgb-d information,” in *Proceedings of the IX Workshop de Visao Computacional, WVC*, 2013.

[38] C.-H. Chuan, E. Regina, and C. Guardino, “American sign language recognition using leap motion sensor,” in *2014 13th International Conference on Machine Learning and Applications*, 2014, pp. 541–544.

[39] L. Rioux-Maldague and P. Giguere, “Sign language fingerspelling classification from depth and color images using a deep belief network,” in *2014 Canadian conference on computer and robot vision*. IEEE, 2014, pp. 92–97.

[40] S. Ameen and S. Vadera, “A convolutional neural network to classify american sign language fingerspelling from depth and colour images,” *Expert Systems*, vol. 34, no. 3, p. e12197, 2017.

[41] Y. LeCun and Y. Bengio, “Convolutional networks for images, speech, and time series,” *The handbook of brain theory and neural networks*, 1998.

[42] R. G. Crespo, E. Verdú, M. Khari, and A. K. Garg, “Gesture recognition of rgb and rgb-d static images using convolutional neural networks,” *IJIMAI*, vol. 5, no. 7, pp. 22–27, 2019.

[43] K. Simonyan and A. Zisserman, “Very deep convolutional networks for large-scale image recognition,” *arXiv preprint arXiv:1409.1556*, 2014.

[44] A. Das, S. Gawde, K. Suratwala, and D. Kalbande, “Sign language recognition using deep learning on custom processed static gesture images,” in *2018 international conference on smart city and emerging technology (ICSCET)*. IEEE, 2018, pp. 1–6.

[45] C. Szegedy, V. Vanhoucke, S. Ioffe, J. Shlens, and Z. Wojna, “Rethinking the inception architecture for computer vision,” in *Proceedings of the IEEE conference on computer vision and pattern recognition*, 2016, pp. 2818–2826.

[46] A. S. M. Miah, J. Shin, M. A. M. Hasan, and M. A. Rahim, “Bensignnet: Bengali sign language alphabet recognition using concatenated segmentation and convolutional neural network,” *Applied Sciences*, vol. 12, no. 8, 2022. [Online]. Available: <https://www.mdpi.com/2076-3417/12/8/3933>

[47] A. M. Rafi, N. Nawal, N. S. N. Bayev, L. Nima, C. Shahnaz, and S. A. Fattah, “Image-based bengali sign language alphabet recognition for

deaf and dumb community,” in *2019 IEEE global humanitarian technology conference (GHTC)*. IEEE, 2019, pp. 1–7.

[48] S. Shorif, M. Ali, F. Jewel, and M. Moni, “KU-BdSL: Khulna University Bengali Sign Language dataset,” 2021. [Online]. Available: <https://data.mendeley.com/datasets/scpvm2nbkm/1>

[49] M. S. Islam, S. S. S. Mousumi, N. A. Jessan, A. S. A. Rabby, and S. A. Hossain, “Isharalipi: The first complete multipurpose open access dataset of isolated characters for bangla sign language,” in *2018 International Conference on Bangla Speech and Language Processing (ICBSLP)*. IEEE, 2018, pp. 1–4.

[50] J. Shin, A. Matsuoka, M. A. M. Hasan, and A. Y. Srizon, “American sign language alphabet recognition by extracting feature from hand pose estimation,” *Sensors*, vol. 21, no. 17, 2021. [Online]. Available: <https://www.mdpi.com/1424-8220/21/17/5856>

[51] F. Zhang, V. Bazarevsky, A. Vakunov, A. Tkachenka, G. Sung, C.-L. Chang, and M. Grundmann, “Mediapipe hands: On-device real-time hand tracking,” *ArXiv*, vol. abs/2006.10214, 2020. [Online]. Available: <https://api.semanticscholar.org/CorpusID:219792872>

[52] G. Ke, Q. Meng, T. Finley, T. Wang, W. Chen, W. Ma, Q. Ye, and T.-Y. Liu, “Lightgbm: A highly efficient gradient boosting decision tree,” *Advances in neural information processing systems*, vol. 30, 2017.

[53] J. Shin, A. S. M. Miah, Y. Akiba, K. Hirooka, N. Hassan, and Y. S. Hwang, “Korean sign language alphabet recognition through the integration of handcrafted and deep learning-based two-stream feature extraction approach,” *IEEE Access*, vol. 12, pp. 68 303–68 318, 2024.

[54] J. Huang, W. Zhou, H. Li, and W. Li, “Sign language recognition using 3d convolutional neural networks,” in *2015 IEEE International Conference on Multimedia and Expo (ICME)*, 2015, pp. 1–6.

[55] H. R. V. Joze and O. Koller, “Ms-asl: A large-scale data set and benchmark for understanding american sign language,” *arXiv preprint arXiv:1812.01053*, 2018.

[56] A. S. M. Miah, M. A. M. Hasan, S.-W. Jang, H.-S. Lee, and J. Shin, “Multi-stream general and graph-based deep neural networks for skeleton-based sign language recognition,” *Electronics*, vol. 12, no. 13, 2023. [Online]. Available: <https://www.mdpi.com/2079-9292/12/13/2841>

[57] O. M. Sincan and H. Y. Keles, “Autsl: A large scale multi-modal turkish sign language dataset and baseline methods,” *IEEE access*, vol. 8, pp. 181 340–181 355, 2020.

[58] W. Zhao, H. Hu, W. Zhou, J. Shi, and H. Li, “Best: Bert pre-training for sign language recognition with coupling tokenization,” in *Proceedings of the Thirty-Seventh AAAI Conference on Artificial Intelligence and Thirty-Fifth Conference on Innovative Applications of Artificial Intelligence and Thirteenth Symposium on Educational Advances in Artificial Intelligence*, ser. AAAI’23/IAAI’23/EAAI’23. AAAI Press, 2023. [Online]. Available: <https://doi.org/10.1609/aaai.v37i3.25470>

[59] S. Patra, A. Maitra, M. Tiwari, K. Kumaran, S. Prabhu, S. Punyeshwarananda, and S. Samanta, “Hierarchical windowed graph attention network and a large scale dataset for isolated indian sign language recognition,” *arXiv preprint arXiv:2407.14224*, 2024.

[60] R. Zuo, F. Wei, and B. Mak, “Natural language-assisted sign language recognition,” in *Proceedings of the IEEE/CVF conference on computer vision and pattern recognition*, 2023, pp. 14 890–14 900.

[61] D. A. SCALE, “Uni-sign: Toward unified sign language un,” *Sign*, vol. 88, pp. 56–3.

[62] R. Xiong, Y. Yang, D. He, K. Zheng, S. Zheng, C. Xing, H. Zhang, Y. Lan, L. Wang, and T. Liu,

“On layer normalization in the transformer architecture,” in *International conference on machine learning*. PMLR, 2020, pp. 10 524–10 533.

[63] S. Takase, S. Kiyono, S. Kobayashi, and J. Suzuki, “On layer normalizations and residual connections in transformers,” *ArXiv*, vol. abs/2206.00330, 2022.

[64] K. Wu, H. Peng, M. Chen, J. Fu, and H. Chao, “Rethinking and improving relative position encoding for vision transformer,” in *Proceedings of the IEEE/CVF international conference on computer vision*, 2021, pp. 10 033–10 041.

[65] D. Hendrycks and K. Gimpel, “Gaussian error linear units (gelus),” *arXiv preprint arXiv:1606.08415*, 2016.

[66] J. Eunice, A. J. Y. Sei, and D. J. Hemanth, “Sign2pose: A pose-based approach for gloss prediction using a transformer model,” *Sensors*, vol. 23, no. 5, 2023. [Online]. Available: <https://www.mdpi.com/1424-8220/23/5/2853>

[67] L. Xiang and Z. Wang, “Joint mixing data augmentation for skeleton-based action recognition,” *ACM Trans. Multimedia Comput. Commun. Appl.*, vol. 21, no. 4, Mar. 2025. [Online]. Available: <https://doi.org/10.1145/3700878>

[68] A. Paszke, S. Gross, F. Massa, A. Lerer, J. Bradbury, G. Chanan, T. Killeen, Z. Lin, N. Gimelshein, L. Antiga et al., “Pytorch: An imperative style, high-performance deep learning library,” *Advances in neural information processing systems*, vol. 32, 2019.

[69] J. Do and M. Kim, “Skateformer: skeletal-temporal transformer for human action recognition,” in *European Conference on Computer Vision*. Springer, 2024, pp. 401–420.

[70] I. Loshchilov and F. Hutter, “Decoupled weight decay regularization,” *arXiv preprint arXiv:1711.05101*, 2017.

[71] Y. Ikuno and Y. Tonomura, “Ubiscription: Finger gesture recognition using smartphone,” 2021.

[72] B. Kwolek, W. Baczyński, and S. Sako, “Recognition of jsl fingerspelling using deep convolutional neural networks,” *Neurocomputing*, vol. 456, pp. 586–598, 2021.

[73] T. Kobayashi, “Classification of japanese signed character with pose estimation and machine learning,” Ph.D. dissertation, Waseda University, 2019.

[74] M. Kakizaki, A. S. M. Miah, K. Hirooka, and J. Shin, “Dynamic japanese sign language recognition throw hand pose estimation using effective feature extraction and classification approach,” *Sensors*, vol. 24, no. 3, 2024. [Online]. Available: <https://www.mdpi.com/1424-8220/24/3/826>

[75] J. Shin, A. S. M. Miah, Y. Akiba, K. Hirooka, N. Hassan, and Y. S. Hwang, “Korean sign language alphabet recognition through the integration of handcrafted and deep learning-based two-stream feature extraction approach,” *IEEE Access*, 2024.

[76] A. S. M. Miah, M. A. M. Hasan, S. Nishimura, and J. Shin, “Sign language recognition using graph and general deep neural network based on large scale dataset,” *IEEE Access*, vol. 12, pp. 34 553–34 569, 2024.

[77] J. Eunice, Y. Sei, and D. J. Hemanth, “Sign2pose: A pose-based approach for gloss prediction using a transformer model,” *Sensors*, vol. 23, no. 5, p. 2853, 2023.